Naftali (Tuli) Herscovici
AnTeg
52 Agnes Drive
Framingham, MA 01901 USA
Tel: +1 (508) 788-5152
Fax: +1 (508) 788-6226
E-mail: tuli@ieee.org

Christos Christodoulou
Department of Electrical and
Computer Engineering
University of New Mexico
Albuquerque, NM 87131-1356 USA
Tel: +1 (505) 277-6580
Fax: +1 (505) 277-1439
E-mail: christos@eece.unm.edu

Uniform Circular Arrays for Smart Antennas

Panayiotis Ioannides and Constantine A. Balanis

Department of Electrical Engineering, Arizona State University
Tempe, AZ 85287-5706
E-mail: balanis@asu.edu

Abstract

As the growing demand for mobile communications constantly increases, the need for better coverage, improved capacity, and higher transmission quality rises. Thus, a more efficient use of the radio spectrum is required. *Smart antenna systems* are capable of efficiently utilizing the radio spectrum and, thus, hold a promise for an effective solution to the present wireless systems' problems, while also achieving reliable and robust high-speed high-data-rate transmission. Although numerous studies for smart antennas have already been conducted using rectilinear arrays, including mostly *uniform linear arrays* (ULAs) and *uniform rectangular arrays* (URAs), not as much effort has been devoted to other configurations. In this paper, the performance of smart antennas with *uniform circular arrays* (UCAs) is examined. A profound justification for this selection is the symmetry possessed by uniform circular arrays. This property provides uniform circular arrays with a major advantage: the ability to scan a beam azimuthally through 360° with little change in either the beamwidth or the sidelobe level. With the use of uniform circular arrays, the two main issues related to smart antennas – estimation of the direction of arrival from incoming signals and beamforming – are both examined.

Keywords: Antenna arrays; adaptive arrays; circular arrays; land mobile radio cellular systems; smart antennas; MUSIC; ESPRIT; direction of arrival estimation; array signal processing

1. Introduction

Smart antennas, or adaptive arrays, have gained great interest among researchers during recent years. Wireless operators are currently searching for new technologies that would be implemented into the existing wireless communications infrastructures to provide broader bandwidth per user channel, better quality, and new value-added services [1]. Such research efforts will enable wireless carriers to maximize the spectral efficiency of their networks so as to meet the explosive growth of the wireless communications industry, and so as to take advantage of the huge market opportunity [2].

Deployed at the base station of the existing wireless infrastructure, smart antennas are capable of bringing outstanding capacity improvement (very important in urban and densely populated areas) to the frequency-resource-limited radio-communications system by an efficient frequency-reuse scheme [1]. This unique feature has been made feasible through the impressive advances in the field of digital signal processing, which enable smart antennas to dynamically tune out interference while focusing on the intended user [3, 4].

With the direction-finding ability of smart antennas, new value-added services, such as *position location* (PL) services for an emergency call, fraud detection, intelligent transportation systems,

law enforcement, accident reporting, etc., are also becoming reality [4-6]. Smart antennas are also deployed in ad hoc networks or wireless local-area networks (WLANs), for example, with mobile *terminals* (notebooks, PDAs, etc.) in a wireless network. The direction-finding ability supports the design of the packet-routing protocol, which decides the manner in which packets are relayed. The beamforming or interference-suppression ability makes it possible to increase the *throughput* at the network nodes, which is limited by interference from neighboring nodes [7, 8].

Until now, the investigation of smart antennas suitable for wireless communication systems has involved primarily rectilinear arrays: *uniform linear arrays* (ULAs) and *uniform rectangular arrays* (URAs). Different algorithms have been proposed for the estimation of the *directions of arrival* (DOAs) of signals arriving at the array, and several adaptive techniques have been examined for the shaping of the radiation pattern under different constraints imposed by the wireless environment. Furthermore, in the literature for adaptive antennas, so far little attention has been paid to circular array topologies, despite their ability to offer a number of advantages. An obvious advantage results from the symmetry of the uniform circular array structure. Due to the fact that a uniform circular array does not have edge elements, directional patterns synthesized with a uniform circular array can be electronically rotated in the plane of the array without significant change in the beam shape.

A key component of smart antenna technology is *adaptive beamforming*, which simultaneously places an antenna radiation pattern beam maximum towards the intended user or *signal of interest* (SOI), and ideally places nulls toward directions of interfering signals or *signals not of interest* (SNOIs). In this letter, we investigate adaptive beamforming with uniform circular arrays. In addition, we compare the beamforming performance of uniform circular and uniform rectangular arrays.

In this paper, we investigate uniform circular arrays for smart-antenna purposes. Two key components of smart-antenna technology examined here are *direction-of-arrival* (DOA) estimation and *adaptive beamforming*. With the former, and the aid of a signal processor, it is feasible to determine the angles from which sources transmit signals towards an antenna array. With the latter, an antenna radiation pattern beam maximum can be simultaneously placed towards the intended user or *signal of interest* (SOI), and, ideally nulls can be placed towards directions of interfering signals or *signals not of interest* (SNOIs). We consider two different approaches for DOA estimation, the MUSIC and the ESPRIT algorithms. For beamforming with uniform circular arrays, we examine both the one-dimensional and two-dimensional cases. For the one-dimensional case, beamforming is performed either along a conical cut for a fixed elevation, or along an elevation for a fixed azimuth. Furthermore, for each beamforming example, the corresponding amplitude and phase excitations of each antenna element of the uniform circular array are provided.

2. Narrowband Beamforming with a Uniform Linear Array

Pattern-synthesis methods with uniform linear arrays have been extensively studied in the context of adaptive beamforming. Whereas the uniform linear array is the simplest array geometry that allows array-processing techniques to be easily applied, it possesses some drawbacks, which lead to the necessity of studying other geometries, as well. Because uniform linear arrays utilize edge elements, all azimuths are not treated equally, and their field-of-view is limited.

To demonstrate this deficiency, and referring to Figure 1, we assume that a uniform linear array is employed at the *base station* (BS) of a wireless communication system for narrowband beamforming applications. During reception, the weighted signals are summed together, producing an output signal that is expressed as [9, 10]

$$y(t,\theta)=\sum_{n=0}^{N-1} w_n x\left(t-n\frac{d}{c}\sin\theta\right), \tag{1}$$

where $x(t)$ is the signal received at the first element, d is the distance between adjacent elements, c is the free-space propagation speed (the speed of light), and θ is the angle of arrival. In the frequency domain, Equation (1) can be written as follows:

$$Y(f,\theta)=\sum_{n=0}^{N-1} w_n X(f) e^{-j2\pi fn\frac{d}{c}\sin\theta}, \tag{2}$$

or

$$H(f,\theta)\triangleq\frac{Y(f,\theta)}{X(f)}=\sum_{n=0}^{N-1} w_n e^{-j2\pi fn\frac{d}{c}\sin\theta}. \tag{3}$$

For narrowband beamforming, f is constant and θ is variable. For the beam to be directed towards the desired direction, θ, the weighting coefficient, w_n, must be set equal to [10]

$$w_n=e^{j2\pi fn\frac{d}{c}\sin\theta_0},\quad n=0,1,\ldots,N-1. \tag{4}$$

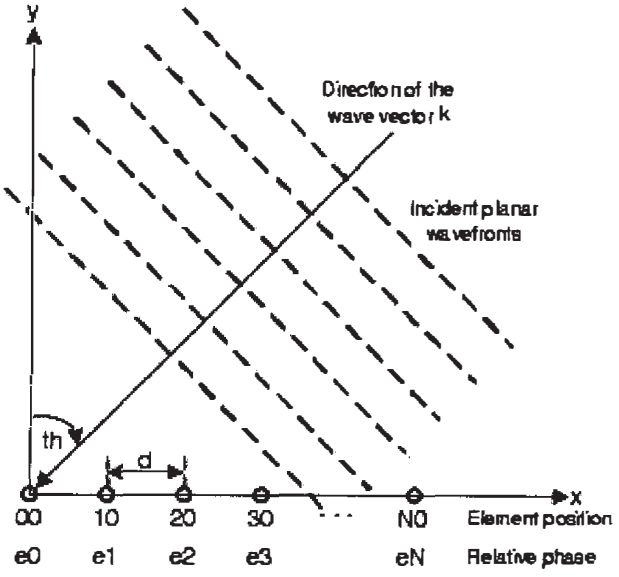

Figure 1. The array response vector for a uniform linear array [11].

In other words, for $\theta = \theta_0$, Equation (3) reduces to

$$H(f,\theta_0) = N, \qquad (5)$$

which is the maximum attainable amplitude obtained by beamforming for complex weights of the same magnitude.

Figure 2a shows the normalized $|H(f,\theta)|$ for a uniform linear array with $N = 8$, $d = c/2f = \lambda/2$, and $\theta_0 = 60°$. As can be seen, a symmetrical pattern appears about the antenna axis ($\theta = \pm 90°$), since $\sin(90° - \theta) = \sin(90° + \theta)$ and $\sin(-90° - \theta) = \sin(-90° + \theta)$. This produces one more undesired main beam towards $\$\theta = 120°$. This is a major drawback in smart-antenna applications since it causes front-back ambiguity. The use of directive elements can eliminate the additional undesired main beam. Typically, the azimuthal field of a uniform linear array must be restricted to a half plane ($\theta \le 180°$). However, in practice the field of view of a uniform linear array is restricted to 120°. To justify this bound, we consider another example of a uniform linear array with $N = 10$, $d = \lambda/2$, and $\theta_0 = 45°$. As shown in the resulting beam pattern of Figure 2b, there is a loss of spatial resolution near the end-fire directions since the sharpness of the beams reduces considerably for $|\theta_0| > 60°$. (Spatial resolution influences the performance of an antenna array. For instance, lower resolution leads to lower directivity of the main beam in beamforming applications, and a reduced ability to separate between two closely spaced signals in direction-of-arrival estimation [12].) For this reason, the angular range of operation for a uniform linear array is restricted to $|\theta_0| \le 60°$ and, therefore, the total angle of coverage is not more than 120°. Moreover, with uniform linear arrays, the beams formed as the array is steered away from boresight broaden significantly [13].

A short-term solution to providing full azimuthal coverage is to use several uniform linear arrays, arranged in a triangular or rectangular shape, as shown in Figure 3, or to rotate the uniform linear array a few times in order to cover the full azimuthal spread [14]. However, the drawback of the former solution is the requirement of using several uniform linear arrays, and hence increasing the cost, as well the collection and processing of additional data.

In general, uniform linear arrays do not provide an appropriate solution to scenarios wherein 360° fields of view are required. In terms of radio propagation, especially in a multipath-rich environment, the signals arrive at the mobile terminal potentially from any azimuthal angle. In these scenarios – which are common in surveillance, cellular phones, etc. – the natural choice is a *uniform circular array* (UCA) [14]. Beyond entire azimuthal coverage, uniform circular arrays can provide a certain degree of source-elevation information (depending on the array's element beam pattern). Note that a uniform rectangular array with non-omnidirectional elements is not able to provide full azimuthal coverage, due to the directional beam pattern of its elements.

Considering mutual coupling, one should expect that circular arrays would suffer more severe effects, since significant coupling can occur between elements located diametrically opposite of each other, in addition to the strong coupling between adjacent elements. However, the basic symmetry of circular arrays has been shown to offer a great ability to compensate for the effects of mutual coupling, by breaking down the array excitation into a series of symmetrical spatial components [14]. Also, this unique feature can deflect directional beams, which remain constant in

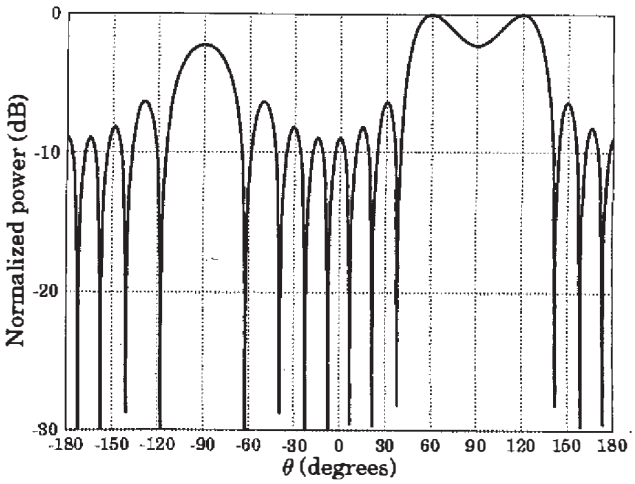

Figure 2a. The directional pattern of the simple narrowband beamformer applied to an eight-element uniform linear array with $d = \lambda/2$ and $\theta_0 = 60°$.

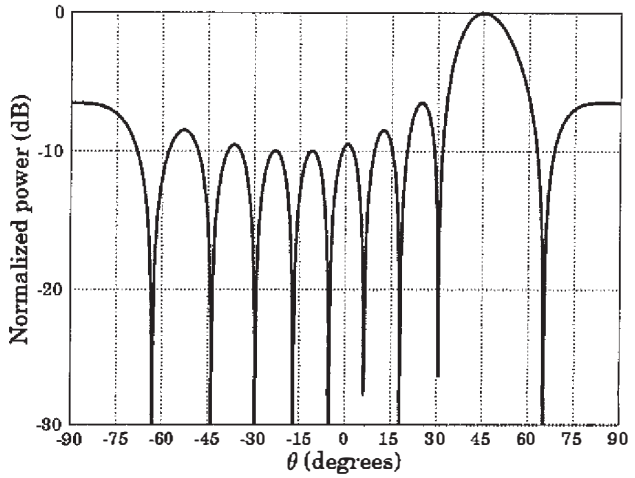

Figure 2b. The directional pattern of the simple narrowband beamformer applied to a 10-element uniform linear array with $d = \lambda/2$ and $\theta_0 = 45°$.

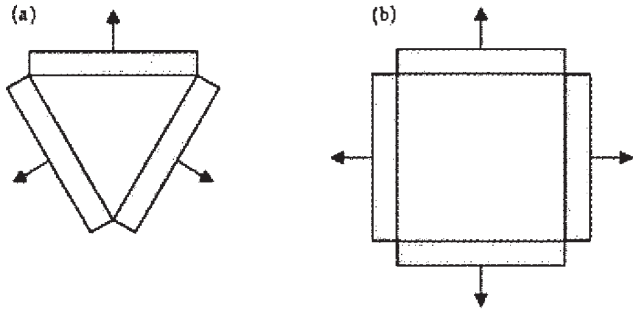

Figure 3. (a) A triangular and (b) a rectangular arrangement of the uniform linear arrays, each covering fields of view of 120° and 90°, respectively.

shape over broad bandwidths. These attractive features, along with new and more convenient methods of array phasing, give powerful advantages to circular arrays for those applications where mutual coupling can limit the performance of the antenna.

Nevertheless, the advantages of uniform circular arrays come at a cost. Many useful array-processing techniques that are derived for uniform linear arrays do not extend directly to uniform circular arrays, due to the mathematical structure of their steering vector not possessing the convenient *Vandermonde* form. (A Vandermonde vector with order n can be written in the form $\left[1, x^1, x^2, ..., x^{n-1}\right]^T$ [15]). In particular, such techniques are

- Dolph-Tschebyscheff beam pattern design [16], and
- spatial smoothing for DOA estimation [17-19].

Other problems uniform circular arrays are challenged to solve include the combating of multipath (introducing highly correlated signal paths) and *multiple access interference* (MAI) mobile environments. As a result, computationally intensive array-processing techniques that are suited for two-dimensional geometries must be employed, such as *maximum likelihood* (ML) methods [20], to deal with such environments.

Circular arrays have been used for many years in the HF band for both communications and direction finding. These systems employed beam co-phased excitation with time-delay compensation to achieve broad-bandwidth operation [21]. The elements were usually monopoles, or a combination of driven and parasitic elements.

3. Circular Array Geometry

Referring to Figure 4, let us assume that a uniform circular array with radius a and consisting of N uniformly distributed antenna elements, assumed to be identical and omnidirectional, is located on the x-y plane and is illuminated by an impinging planar wavefront. A spherical coordinate system is used to represent the arrival directions from incoming plane waves. The origin of the coordinate system is located at the center of the array. Source elevation angles, $\theta \in [0, \pi/2]$, are measured from the z axis, and azimuth angles, $\phi \in [0, 2\pi]$, are measured counterclockwise from the x axis on the x-y plane.

The angular position of the nth element of the array is given by [10]

$$\phi_n = 2\pi\left(\frac{n}{N}\right), \quad n = 1, 2, ..., N. \tag{6}$$

The narrowband planar wave with wavelength λ (and corresponding wavenumber $k = 2\pi/\lambda$) arrives at the antenna from elevation angle θ and azimuthal angle ϕ. The unit vector $\hat{\mathbf{a}}_r$ from the origin is represented in Cartesian coordinates by

$$\hat{\mathbf{a}}_r = \hat{\mathbf{a}}_x \sin\theta\cos\phi + \hat{\mathbf{a}}_y \sin\theta\sin\phi + \hat{\mathbf{a}}_z \cos\theta. \tag{7}$$

The unit vector $\hat{\mathbf{a}}_{pn}$ from the origin to the nth element of the array is written as

$$\hat{\mathbf{a}}_{pn} = \hat{\mathbf{a}}_x \cos\phi_n + \hat{\mathbf{a}}_y \sin\phi_n, \quad n = 1, 2, ..., N. \tag{8}$$

The vector $\Delta\mathbf{r}_n$ represents the differential distance by which the planar wavefront reaches the nth element of the array relative to the origin, and it is given by [10]

$$\Delta\mathbf{r}_n = \hat{\mathbf{a}}_r a\cos\psi_n. \tag{9}$$

Since the wavefront is incoming and not radiating outwards, ψ_n can be expressed as

$$\begin{aligned}\cos\psi_n &= -\hat{\mathbf{a}}_r \cdot \hat{\mathbf{a}}_{pn} \\ &= -\left(\hat{\mathbf{a}}_x \sin\theta\cos\phi + \hat{\mathbf{a}}_y \sin\theta\sin\phi + \hat{\mathbf{a}}_z \cos\theta\right) \\ &\quad \cdot\left(\hat{\mathbf{a}}_x \cos\phi_n + \hat{\mathbf{a}}_y \sin\phi_n\right) \\ &= -\left(\sin\theta\cos\phi\cos\phi_n + \sin\theta\sin\phi\sin\phi_n\right) \\ &= -\sin\theta\left(\cos\phi\cos\phi_n + \sin\theta\sin\phi_n\right) \\ &= -\sin\theta\cos\left(\phi - \phi_n\right), \quad n = 1, 2, ..., N,\end{aligned} \tag{10}$$

and, therefore, Equation (9) reduces to [10]

$$\Delta\mathbf{r}_n = -\hat{\mathbf{a}}_r a\sin\theta\cos\left(\phi - \phi_n\right), \quad n = 1, 2, ..., N. \tag{11}$$

Furthermore, assuming that the wavefront passes through the origin at time $t = 0$, it impinges on the nth element of the array at the relative time of

$$\tau_n = -\frac{a}{c}\sin\theta\cos\left(\phi - \phi_n\right), \quad n = 1, 2, ..., N, \tag{12}$$

where c is the speed of light in free space. Positive time delay indicates that the wavefront impinges on the nth element after it passes through the origin, whereas negative time delay indicates that the wavefront impinges on the nth element before it arrives at the origin. Moreover, based on Equation (10), the element-space circular-array *steering vector* is given by

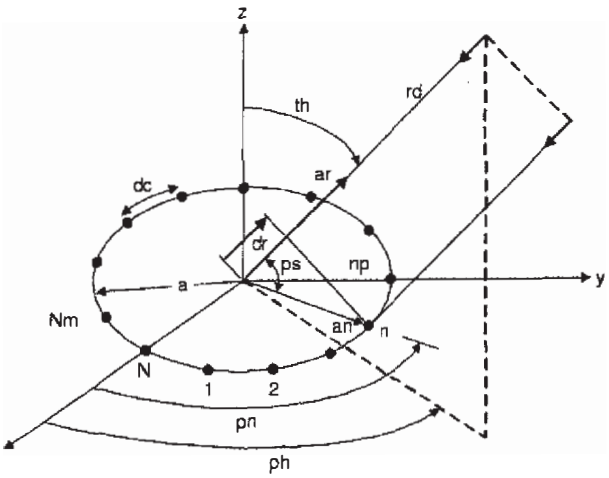

Figure 4. The geometry of a circular array with radius a and N equally spaced elements, along with an impinging planar wavefront.

$$\mathbf{a}(\boldsymbol{\theta}) = \mathbf{a}(\varsigma,\phi) = \left[e^{\varsigma\cos(\phi-\phi_1)}, e^{\varsigma\cos(\phi-\phi_2)}, \ldots, e^{\varsigma\cos(\phi-\phi_N)} \right]^T, \quad (13)$$

where the elevation dependence is through the parameter $\varsigma = ka\sin\theta$, and the vector $\boldsymbol{\theta} = (\varsigma,\phi)$ is used to represent source arrival directions.

The dominant method in analyzing circular arrays is through the so-called *phase-mode excitation*}, which is essentially the decomposition of the array excitation function into different Fourier harmonics by using Fourier analysis. It stems from the fact that the beam pattern of the uniform circular array is periodic in azimuth [21].

4. Direction-of-Arrival Estimation with Uniform Circular Arrays

In this section, we consider the computation of the *directions of arrival* (DOAs) of signals transmitted towards uniform circular arrays by several sources. So far, several algorithms have been proposed in the literature for the two-dimensional angle estimation (azimuth and elevation) of multiple plane waves incident on a uniform circular array.

4.1 Real Beam-Space MUSIC for Circular Arrays

As with other array geometries, a major category in the context of DOA estimation with uniform circular arrays relies on the *MUltiple SIgnal Classification* (MUSIC) algorithm, which utilizes the fact that signal vectors are orthogonal to the noise subspace. MUSIC offers numerous advantages over element-space operation, including reduced computation, since subspace estimates are obtained via real-valued eigen decompositions, and enhanced performance in correlated-source scenarios, due to the attendant forward-backward averaging effect [22]. An interesting version of the MUSIC algorithm is the Real Beam-space MUSIC algorithm for uniform circular arrays (UCA-RB-MUSIC). The complete development of the algorithm can be found in [22].

4.1.1 Simulation Results of Direction Finding with the UCA-RB-MUSIC Algorithm

In order to test the UCA-RB-MUSIC algorithm, we considered two examples with different array geometries and different numbers of sources, as shown in Table 1. The corresponding UCA-RB-MUSIC power spectrum for these two cases is displayed in Figures 5a and 5b, respectively. The performance of the UCA-RB-MUSIC was indeed excellent, since very sharp peaks appeared in the directions of arriving signals.

4.1.2 Comparison of Classical MUSIC with the UCA-RB-MUSIC Algorithm

The classical MUSIC algorithm is a very popular high-resolution algorithm, applicable to arrays of arbitrary but known configuration and response [23, 24]. An interesting investigation is to compare the classical MUSIC algorithm with the UCA-RB-MUSIC algorithm, developed exclusively for uniform circular arrays. To compare these two algorithms, we considered the signals and geometries of Table 2, where the impinging signals were assumed to arrive from an elevation identical to the plane of the array ($\theta = \pi/2$).

The corresponding power spectra for these two cases are shown in Figures 6a and 6b, respectively. For the first case, both of the algorithms had great performance, with that of the UCA-RB-MUSIC algorithm being slightly better (sharper peaks). This is justified by the fact that while the classical MUSIC algorithm is applicable to every possible array geometry, the UCA-RB-MUSIC was explicitly developed for uniform circular arrays, and fully exploits the array structure. However, for the second case, we observed that while the performance of the classical MUSIC was

Table 1a. The geometries used to test the UCA-RB-MUSIC algorithm.

	Case 1	Case 2
Number of elements	$N = 8$	$N = 10$
Radius of the UCA	$a = 0.6\lambda$ $(d_c = 0.4127\lambda)$	$a = 0.75\lambda$ $(d_c = 0.4712\lambda)$
Number of impinging sources	$K = 3$	$K = 4$
SNR per equal-power source	10 dB	10 dB
Number of collected samples	3000	4000

Table 1b. The directions of arrival of the signals used to test the UCA-RB-MUSIC algorithm.

Case 1	Case 2
$\theta_1 = 30°, \phi_1 = 120°$	$\theta_1 = 30°, \phi_1 = 300°$
$\theta_2 = 45°, \phi_2 = 210°$	$\theta_2 = 45°, \phi_2 = 150°$
$\theta_3 = 60°, \phi_3 = 300°$	$\theta_3 = 60°, \phi_3 = 240°$
	$\theta_4 = 75°, \phi_4 = 60°$

DOCKET ALARM

Explore Litigation Insights

Docket Alarm provides insights to develop a more informed litigation strategy and the peace of mind of knowing you're on top of things.

Real-Time Litigation Alerts

Keep your litigation team up-to-date with **real-time alerts** and advanced team management tools built for the enterprise, all while greatly reducing PACER spend.

Our comprehensive service means we can handle Federal, State, and Administrative courts across the country.

Advanced Docket Research

With over 230 million records, Docket Alarm's cloud-native docket research platform finds what other services can't. Coverage includes Federal, State, plus PTAB, TTAB, ITC and NLRB decisions, all in one place.

Identify arguments that have been successful in the past with full text, pinpoint searching. Link to case law cited within any court document via Fastcase.

Analytics At Your Fingertips

Learn what happened the last time a particular judge, opposing counsel or company faced cases similar to yours.

Advanced out-of-the-box PTAB and TTAB analytics are always at your fingertips.

API

Docket Alarm offers a powerful API (application programming interface) to developers that want to integrate case filings into their apps.

LAW FIRMS
Build custom dashboards for your attorneys and clients with live data direct from the court.

Automate many repetitive legal tasks like conflict checks, document management, and marketing.

FINANCIAL INSTITUTIONS
Litigation and bankruptcy checks for companies and debtors.

E-DISCOVERY AND LEGAL VENDORS
Sync your system to PACER to automate legal marketing.